

Final Report for Period: 09/2009 - 08/2010**Submitted on:** 11/29/2010**Principal Investigator:** Yoda, Minami .**Award ID:** 0625865**Organization:** GA Tech Res Corp - GIT**Submitted By:**

Yoda, Minami - Principal Investigator

Title:

NSF/Sandia: Novel Thermometry Techniques and Nanostructured Surfaces to Enhance Micro- and Meso-Scale Thermal Management Technologies

Project Participants**Senior Personnel****Name:** Yoda, Minami**Worked for more than 160 Hours:** Yes**Contribution to Project:****Name:** Joshi, Yogendra**Worked for more than 160 Hours:** Yes**Contribution to Project:****Post-doc****Graduate Student****Name:** Dietz, Carter**Worked for more than 160 Hours:** Yes**Contribution to Project:**

Performed heat transfer studies for microchannels with and without carbon nanotube-encrusted surfaces for his Master's thesis (expected August 2007).

Name: Kim, Myeongsub**Worked for more than 160 Hours:** Yes**Contribution to Project:**

Evaluating temperature sensitivity of PbS infrared quantum dots for his doctoral thesis.

Name: Suda-Cederquist, Keith**Worked for more than 160 Hours:** Yes**Contribution to Project:**

Master's thesis student who was involved during the first quarter of the first year of this project. Graduated in Spring semester 2007.

Undergraduate Student**Technician, Programmer****Other Participant****Research Experience for Undergraduates****Organizational Partners**

Other Collaborators or Contacts

Dr. Yoda worked with the group of Prof. Mounji Bawendi in the Department of Chemistry at MIT. Scott Geyer, a doctoral student in Dr. Bawendi's lab, provided us with lead sulfide (PbS) infrared quantum dot (QD) samples, including both PbS QD 'cores' and CdS-overcoated PbS core QD.

In 2008, Dr. Joshi has hosted Mr. Yunhyeok Im in his laboratory as a Visiting Research Scholar partially supported by the Korea Science and Engineering Foundation (KOSEF). Mr. Im, who was on leave from Samsung while he pursued his doctoral studies at the Korea Advanced Institute of Science and Technology (KAIST), has been instrumental in the development of the copper nanowire growth process used in this work to fabricate superhydrophobic surfaces. Dr. Joshi has also been appointed an adjunct faculty member at KAIST as a result of this collaboration.

Activities and Findings

Research and Education Activities: (See PDF version submitted by PI at the end of the report)

Findings: (See PDF version submitted by PI at the end of the report)

Training and Development:

This project educated three graduate students, K. Suda-Cederquist, C. Dietz (both American citizens) and M. Kim, in experimental heat transfer and optical thermometry techniques.

Mr. Suda-Cederquist, who received his Master's thesis on the initial development of evanescent-wave fluorescence thermometry, performed temperature calibrations to measure the temperature sensitivity of fluorescein illuminated by evanescent waves. During this research, he learned about microscopy, digital imaging and image processing, and fluorescence.

Mr. Dietz learned to grow copper nanowires using a low-temperature electroplating process, and learned a variety of microfabrication skills. He also became familiar with contact-line dynamics, superhydrophobicity, and condensation processes, as well as environmental scanning electron microscopy and high-speed visualization. Mr. Dietz is currently working at Sandia National Laboratories.

For his doctoral studies, Mr. Kim has learned how to fabricate glass substrates with thin-film indium tin oxide (ITO) heaters as well as PDMS and acrylic channels. He has also become an expert on a variety of optical microscopy techniques including total internal reflection fluorescence microscopy, digital imaging and image processing. He will be completing his doctorate at the end of calendar year 2010, and is planning to become a postdoctoral researcher at the University of Victoria in Canada.

Outreach Activities:

As detailed in the activities section, Drs. Yoda and Joshi have been involved in mentoring local high school students in summer research, including a female high school student who worked with graduate student C. R. Dietz on fabricating copper nanostructured surfaces.

Dr. Yoda has also started a program to involve high school students in summer research with faculty in the School of Mechanical Engineering at Georgia Tech. The first summer of this program (2010) brought seven students, including four female students, between their Junior and Senior years to work with four ME faculty, and we plan to have this program every summer.

Journal Publications

Dietz, CR; Joshi, YK, "Single-phase forced convection in microchannels with carbon nanotubes for electronics cooling applications", NANOSCALE AND MICROSCALE THERMOPHYSICAL ENGINEERING, p. 251, vol. 12, (2008). Published, 10.1080/1556726080217193

Kim, M; Yoda, M, "Dual-tracer fluorescence thermometry measurements in a heated channel", EXPERIMENTS IN FLUIDS, p. 257, vol. 49, (2010). Published, 10.1007/s00348-010-0853-

M. Kim; M. Yoda, "Fluorescence thermometry for measuring wall and bulk liquid temperatures", Journal of Heat Transfer Transactions of the ASME, p. , vol. , (2010). Submitted,

M. Kim; M. Yoda, "Infrared quantum dots for liquid-phase thermometry in silicon", Measurement Science and Technology, p. , vol. , (2010). Submitted,

Dietz, C; Rykaczewski, K; Fedorov, AG; Joshi, Y, "Visualization of droplet departure on a superhydrophobic surface and implications to heat transfer enhancement during dropwise condensation", APPLIED PHYSICS LETTERS, p. , vol. 97, (2010). Published, 10.1063/1.346027

Dietz, C; Rykaczewski, K; Fedorov, A; Joshi, Y, "ESEM Imaging of Condensation on a Nanostructured Superhydrophobic Surface", JOURNAL OF HEAT TRANSFER-TRANSACTIONS OF THE ASME, p. , vol. 132, (2010). Published, 10.1115/1.400175

Im, Y., Joshi, Y., Dietz, C. and Lee, S. S., "Enhanced boiling of a dielectric liquid on copper nanowire surfaces", International Journal of Micro-Nano Scale Transport, p. 79, vol. 1, (2010). Published,

Books or Other One-time Publications

Carter R. Dietz, "Single-Phase Forced Convection in a Microchannel with Carbon Nanotubes for Electronic Cooling Applications", (2007). Thesis, Published

Bibliography: M. S. thesis, Georgia Institute of Technology

M. Kim; M. Yoda, "Fluorescence thermometry for measuring wall surface and bulk fluid temperatures", (2010). Conference paper, Published Collection: Proceedings of the 14th International Heat Transfer Conference (Washington, DC)

Bibliography: ASME paper IHTC14-22884

M. Kim; M. Yoda, "Using quantum dots for liquid-phase thermometry at near-infrared wavelengths in silicon devices", (2010). Conference paper, Published

Collection: Proceedings of the 14th International Heat Transfer Conference (Washington, DC)

Bibliography: ASME paper IHTC14-22885

Web/Internet Site

Other Specific Products

Contributions

Contributions within Discipline:

We continue to make good progress towards developing thermometry techniques suitable for microfluidics devices and understanding how superhydrophobic surfaces could affect condensation. Specific contributions include:

- 1) The PIs have shown that two-color fluorescence thermometry based on fluorescein and sulforhodamine B (instead of the more commonly used rhodamine B and rhodamine 110) can be used to measure water temperature fields at a spatial resolution of 30 μm with an accuracy, based on comparisons with numerical simulations, of 0.35 $^{\circ}\text{C}$. The PIs have also shown that evanescent-wave fluorescence thermometry (EFT) based on the emissions from fluorescein can be used to measure wall surface temperature fields at a spatial resolution of 10 μm with an accuracy, based on comparisons with numerical simulations, of 0.6 $^{\circ}\text{C}$.
- 2) The PIs have fabricated superhydrophobic nanostructured surfaces from copper using a low-temperature process which does not require specialized cleanroom facilities suitable for microscale condensers. They have shown, using environmental scanning electron microscopy to visualize the condensation of water on these surfaces, that these nanostructured superhydrophobic surfaces continuously form drops in the size range (less than 10 μm diameter) that contribute the most to condensation heat transfer, and that these drops also continuously roll off the

surface. In contrast, ESEM visualizations of condensation on non-structured (i.e., smooth) hydrophobic surfaces show that the smooth surfaces only form such small drops in the initial phases of condensation, and that the smooth surface later becomes completely flooded by condensate.

3) The PIs have also shown that CdS-overcoated PbS infrared quantum dots can be used as to measure liquid temperature fields, albeit in toluene, in monolithic silicon devices, and that these tracers have a temperature sensitivity, measured in terms of the change in their emission intensity, of -0.5% per degree C.

Contributions to Other Disciplines:

The work on superhydrophobic surfaces has the potential to lead to improved compact efficient heat exchangers. Extrapolations based on classic theories of dropwise condensation suggest that such nanostructured surfaces, when vertically oriented, would have a 100% greater heat transfer coefficient compared with a vertical non-structured surface under similar conditions.

The work on thermometry techniques has the potential to lead to new designs for single-phase liquid and two-phase evaporative heat exchangers. Given that controlling the temperature of aqueous solutions such as blood plasma and urine is critical in a variety of microfluidics-based medical devices, these techniques also have the potential to improve designs of medical diagnostic devices.

Contributions to Human Resource Development:

This project has educated three graduate students, including two US citizens. It has resulted in three Master's degrees in Mechanical Engineering, and will shortly result in one doctorate. The project has also exposed one female undergraduate student, E. L. Elbel, and one female high school student, A. Bhatia, to research.

Contributions to Resources for Research and Education:

The PIs have worked with science teachers at a local high school, Westminster High School, to create a new program involving students between their Junior and Senior years in research projects with various faculty in the School of Mechanical Engineering at Georgia Tech. In the first summer (2010), four female and three male students from Westminster and Paces Academy worked with four different GT ME faculty. We plan to hold this high school research program every summer.

Contributions Beyond Science and Engineering:

Conference Proceedings

Kim, M;Yoda, M, INFRARED QUANTUM DOTS FOR LIQUID-PHASE THERMOMETRY IN SILICON MICROCHANNELS, "AUG 10-14, 2008", HT2008: PROCEEDINGS OF THE ASME SUMMER HEAT TRANSFER CONFERENCE, VOL 1, : 349-355 2009

Categories for which nothing is reported:

Organizational Partners

Any Web/Internet Site

Any Product

Contributions: To Any Beyond Science and Engineering

Research Activities

This grant is a collaboration between Profs. Minami Yoda and Yogendra Joshi in the George W. Woodruff School of Mechanical Engineering at the Georgia Institute of Technology (GT). The final report summarizing the work performed under this grant covers the period from September 2006 through August 2010.

In 1965, Gordon Moore of Intel predicted that the density of transistors on a computer chip would double every two years. Since then, the microelectronics industry has managed to follow Moore's Law, with a doubling in component density every 18–24 months. This exponential growth in component density, however, has created huge thermal management challenges as more and more transistors (*e.g.* the 2006 Intel dual-core Itanium 2 contains 1.7 billion transistors) dissipate more and more heat. Chip average heat fluxes are projected to exceed 100 W/cm^2 within a decade,¹ with local heat fluxes over hot spots with areas of about $500 \mu\text{m}^2$ up to an order of magnitude greater than this value. Even with the latest advances in heat sinks, forced-air cooling cannot dissipate heat fluxes of this magnitude, while meeting the necessary size restrictions. There is thus an urgent need to develop compact single- or two-phase thermal management technologies with micron-scale addressability that can handle heat fluxes up to 1 kW/cm^2 .

The objectives of this research are therefore to enable new thermal management technologies by developing: 1) novel non-intrusive high-spatial resolution thermometry techniques to measure surface and coolant temperatures in complex microscale geometries and through silicon surfaces; and 2) new mesoscale technologies incorporating microchannels with nanostructured surfaces for enhanced convective heat transfer. Over the four-year period (including a one-year no-cost extension) of this grant, we have:

- developed a dual-tracer fluorescent thermometry (DFT) technique with more than triple the sensitivity of previous techniques to measure liquid-phase temperatures in Poiseuille flow through a heated channel with a spatial resolution as fine as $3.7 \mu\text{m}$ and experimental uncertainties as small as 0.2°C (at a spatial resolution of $30 \mu\text{m}$);
- developed evanescent-wave fluorescence thermometry (EFT), a technique that can measure water temperatures over the first 300 nm next to the wall, and verified using numerical simulations that these data are effectively the wall surface temperature, even in the presence of strong wall-normal temperature gradients;
- fabricated superhydrophobic surfaces with nanoscale roughness consisting of an array of copper (Cu) nanowires thermally coupled to a silicon (Si) substrate and performed high-speed visualizations of the initial phases of the condensation of water on superhydrophobic and bare Si surfaces under vacuum in an environmental scanning electron microscope (ESEM);
- demonstrated that the emissions in the near-infrared from nanocrystals, or “quantum dots” of the semiconductor lead sulfide (PbS) suspended in toluene are temperature-

¹ www.itrs.net/Links/2006Update/2006UpdateFinal.htm

sensitive, decreasing in intensity by about 0.5% for every °C increase in the suspension temperature.

Summaries of the research activities for these topics follow.

Dual-Tracer Fluorescence Thermometry in Heated Channels

Cooling the next generation of microelectronics with heat fluxes of more than 1 kW/cm² over hot spots with typical dimensions of less than 100 μm will require new single- and two-phase thermal management technologies with micron-scale addressability. Although the (mainly laminar) thermal transport in compact heat exchangers can be numerically simulated, these simulations will require significant computational time because of the geometric complexity of these designs and spatial variations in heat flux due to chip “power maps,” *i.e.*, the power dissipation profile.

Estimating coolant temperature distributions using reduced-order models, which predict thermal performance using heat transfer correlations and/or coarser scale models, may therefore be a more efficient approach for the initial design and optimization of new microscale thermal management technologies. It is unclear, however, if classic convective heat transfer correlations are valid for microchannel networks because of significant thermal coupling between the channels due to heat spreading via the high thermal conductivity silicon (Si).

By Newton’s Law of Cooling, the local heat flux normal to the surface is proportional to the difference between the local wall surface and mean (bulk) fluid temperatures T_s and T_m , respectively. Developing local heat transfer correlations for microscale geometries therefore requires accurately measurement of wall surface and bulk temperature fields with a spatial resolution of $O(1\ \mu\text{m})$.

Intensity-based fluorescence thermometry (FT) is typically used to estimate water temperature fields based on variations in the emission intensity of an aqueous fluorophore solution. In DFT, the accuracy of FT is improved by taking the ratio of the emission signals from two different fluorophores to eliminate variations in the signal due to (spatial and temporal) variations in the excitation intensity.² The DFT studies used two temperature-sensitive fluorophores, fluorescein (Fl) and sulforhodamine B (SrB), with emission intensities that increase and decrease, respectively, with increasing temperature,³ were used to further improve the accuracy of the measurements. Based on our calibrations for a 5 μmol/L Fl, 5 μmol/L SrB and 7 mmol/L sodium tetraborate (Na₂B₄O₇) solution, the temperature sensitivity of the ratio of the Fl to SrB signals increases from 3% to 10% per °C as the solution temperature T increases from 20 °C to 60 °C, respectively, *vs.* The ratio of the Fl to SrB emissions therefore gives a temperature sensitivity significantly greater than the 1.7% decrease per °C increase reported for the more common DFT pair of rhodamine B and rhodamine 110.⁴

² J. Coppeta and C. Rogers (1998) “Dual emission laser induced fluorescence for direct planar scalar behavior measurements” *Exp. Fluids* **23**, 1

³ M. B Shafii, C. L. Lum and M. M. Koochesfahani (2010) “In-situ LIF temperature measurements in aqueous ammonium chloride solution during uni-directional solidification” *Exp. Fluids* **48**, 651

⁴ J. Sakakibara and R. J. Adrian (1999) “Whole field measurement of temperature in water using two-color laser induced fluorescence” *Exp. Fluids* **26**, 7

Liquid temperatures were measured in the steady Poiseuille flow of a FI/SrB solution through a 1 mm square PDMS-glass channel at Reynolds numbers based on the channel cross-sectional dimension and average speed $Re = 3.3$ and 8.3 (Fig. 1). The channel, which was fabricated at GT, was heated by 20 mW of electrical power supplied to an indium tin oxide (ITO) heater (nominal dimensions $7 \text{ mm} \times 1 \text{ mm} \times 300 \text{ nm}$) deposited on the glass bottom wall of the channel 1 mm from the side wall of the channel. The FI/SrB solution was excited over the entire cross-section of the channel with light from an argon-ion laser at a wavelength $\lambda = 514 \text{ nm}$, and the emissions from the flowing fluid near the bottom glass wall near the ITO heater were imaged and recorded by an electron multiplying CCD (EMCCD) camera. The average uncertainty in the temperatures measured by the DFT technique was estimated to be $1.4 \text{ }^\circ\text{C}$ and $0.21 \text{ }^\circ\text{C}$ at spatial resolutions of $3 \text{ }\mu\text{m}$ and $30 \text{ }\mu\text{m}$, respectively.

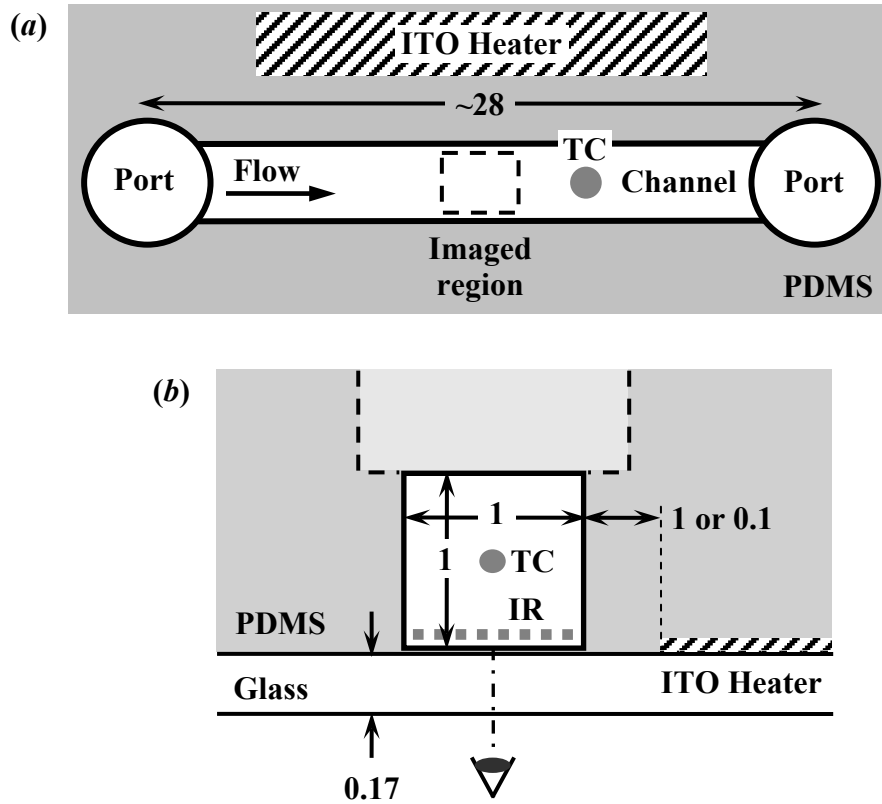


Figure 1 (a) Top and (b) side views of the 1 mm square PDMS-glass channel with an ITO heater. The shaded rectangle and line indicate the region imaged by the microscope objective in the top and side views (IR), respectively. A thermocouple (TC) downstream of the imaged region is used to monitor the liquid temperature. Flow is out of the page in (b). All dimensions are given in mm.

The FT results were validated by 3D finite-volume simulations of steady laminar flow using the commercial CFD software package FLUENT v6.2 of the PDMS-glass channel, including the ITO heater. Standard empirical free-convection boundary conditions for external flows were imposed on the surfaces exposed to ambient conditions, and a constant heat-generation rate boundary condition was imposed at the ITO heater. In all the simulations, the FLUENT predictions were consistent with the TC readings (averaged over the TC bead diameter of 0.3 mm) obtained in the Poiseuille flow experiments.

Limitations on the RAM on the personal computer used for these computations, which was limited to 3.5 GB, limited the finest spatial resolution of these simulations to 50 μm .

Evanescent-Wave Fluorescence Thermometry in Heated Channels

When light undergoes total internal reflection at a refractive-index (*e.g.* glass-water) interface, evanescent waves are generated in the lower refractive index medium (here, water). Evanescent waves have an intensity that is maximum at, and decays exponentially with distance normal to, the interface with a length scale, the penetration depth z_p , which is typically $O(100\text{ nm})$. Evanescent waves therefore are uniquely well-suited to probing the first few hundred nanometers next to the wall.

However, because evanescent waves have their maximum intensity at the interface, even a small amount of adsorbed fluorophore has a significant effect on the accuracy and reproducibility of the fluorescence thermometry data. Of the two fluorophores used in the DFT studies, FI had negligible adsorption on either PDMS or glass surfaces. Sulforhodamine B, however, had enough absorption that the evanescent-wave fluorescence thermometry (EFT) studies only used the temperature-sensitive tracer FI, specifically 30 $\mu\text{mol/L}$ FI and 0.1 mol/L phosphate buffer at pH 8.5. Calibrations showed that the emissions from FI excited by evanescent waves increased by 1.8% per $^{\circ}\text{C}$ increase in solution temperature.

Liquid temperatures were measured in the steady Poiseuille flow through a PDMS-glass channel similar to that shown in Fig. 1 except that the ITO heater was 0.1 mm (*vs.* 1 mm in the DFT studies) from the channel side wall. The FI solution was illuminated by evanescent waves with $z_p \approx 80\text{ nm}$ generated by the objective of a TIR fluorescence microscope at $\lambda = 514\text{ nm}$, and the emissions were imaged and recorded by the same EMCCD camera. The region imaged by the camera was estimated to be $4z_p$, or the first 320 nm next to the wall. The average uncertainty in the EFT temperatures was estimated to be 1.1 $^{\circ}\text{C}$ and 0.16 $^{\circ}\text{C}$ at spatial resolutions of 1 μm and 10 μm , respectively. The EFT results were compared with numerical predictions for the wall surface temperature obtained from the simulations described in the previous section.

Fabrication of and Visualizations of Condensation on Superhydrophobic Surfaces

Since there is a wide selection of materials and methods to fabricate superhydrophobic surfaces, a set of criteria were outlined to help narrow the focus of potential structures. Ideally, the fabrication of a superhydrophobic surface should have a low-cost, high through-put method of production, be easy to scale up, and have compatibility with current condenser design and materials. To this end, cupric hydrophobic $[\text{Cu}(\text{OH})_2]$ and copper oxide $[\text{CuO}]$ nanostructures were selected.

$\text{Cu}(\text{OH})_2$ and CuO nanostructures were formed by alkali surface oxidation of a copper source. On account of its high thermal conductivity, relatively low cost, and ease in machining, copper is the standard material for current commercial condensing coils, making these nanostructures ideal for integration into current condenser designs. The alkali surface oxidation process is performed at room temperature and does not require special equipment. The nanostructures self assemble using a solution of sodium hydroxide and ammonium persulfate following chemical reactions (A) and (B):





Table 1 gives the concentrations and submersion times for the two different structures. All processes were carried out with a total volume of 50 mL. Figure 2 depicts the geometry and differences between these two structures.

To reduce the surface energy of the nanostructures, the nanostructured surfaces were modified with a hydrophobic promoter. For this process, a 20 nm coating of gold was sputtered onto the structures. The structures were then submerged in 1-hexadecanethiol for 1 s, then rinsed thoroughly with acetone to remove excess 1-hexadecanethiol, and soaked in ethanol for 48 h to dissolve any residual 1-hexadecanethiol. After soaking, the structures were removed and allowed to dry.

The sessile drop technique was used to quantify the superhydrophobicity of the surfaces. In this technique, a liquid drop is placed on the surface, and the contact angle is measured visually with a goniometer. The contact angle for a 4 μL drop of water on the Cu(OH)_2 structures was found to be 155° with a hysteresis of 1° , while the contact angle on the CuO structures was found to be 159° with a hysteresis of 2° . These measurements clearly demonstrate that both surfaces were superhydrophobic.

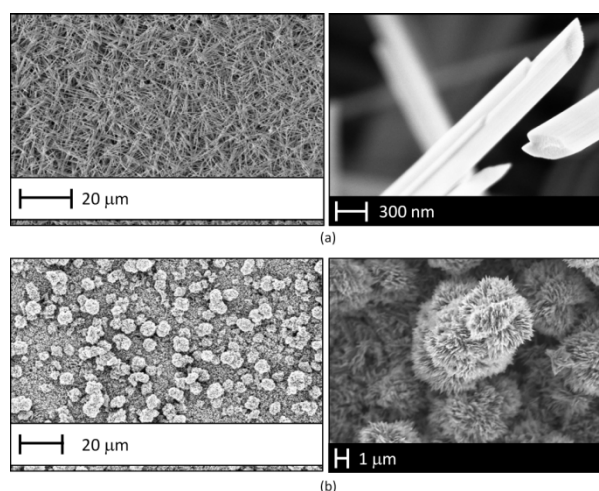


Figure 2 Scanning electron microscopy (SEM) image of (a) Cu(OH)_2 and (b) CuO nanostructures.

Table 1 Fabrication parameters for the two different superhydrophobic nanostructured surfaces.

	NaOH Concentration (M)	$(\text{NH}_4)_2\text{S}_2\text{O}_8$ Concentration (M)	Submersion Time (h)	NaOH Source	Stirring Time Before Submersion (h)
Cu(OH)_2	2.5	0.088	0.5	50% (w/w)	15
CuO	2.5	0.1	1	Pellets	0

An *in situ* investigation of water condensing upon the superhydrophobic Cu(OH)_2 structures was then conducted in an environmental scanning electron microscope (ESEM) to obtain high-resolution visualizations of the condensation process. This visualization gives a qualitative understanding of the condensation process and provides evidence of

whether the condensate is in the Wenzel or Cassie regimes. A quantitative assessment of the condensation process can also be obtained from these visualization studies by tallying the number and diameters of the condensed drops as a function of time. The superhydrophobic surface was compared to a non-structured hydrophobic surface to evaluate the potential heat transfer enhancement due to dropwise condensation. The non-structured surface was a silicon substrate that was coated with Rain-X to increase the contact angle from 65° to 91°. The Cu(OH)₂ structures, which were attached to a 10 mm by 10 mm silicon die for mechanical support, were found to have smaller rolling drops and a higher sweeping frequency than the non-structured surface, presumably due to the reduced surface energy of the structured superhydrophobic surface. Since, most of the heat transfer during dropwise condensation is associated with droplets less than 10 μm in diameter, the increased sweeping frequency should lead to enhanced heat transfer during dropwise condensation.

During imaging, the water vapor pressure in the ESEM chamber was maintained at 5.8 Torr, and the stage temperature was reduced to 268K. The stage temperature was measured with a T-type thermocouple located between the cold side of the thermoelectric device and the silicon substrate. The stage was tilted to a 30° angle from the horizontal. Videos were recorded at 1 Hz for 4 min over a field of view of 100 μm square, and every other frame was saved as an image for post-processing. The number of droplets in every fifth image (*i.e.*, every 10 s) and the diameter of each droplet were measured. The experiments were replicated four times at different locations on the sample.

Infrared Quantum Dot Thermometry through Silicon Surfaces

Most optically based liquid thermometry techniques including FT exploit temperature-sensitive changes in the properties (*e.g.* intensity, lifetime) of the photoluminescent (PL) emissions of various tracers suspended or dissolved in the liquid. However, nearly all of these emissions are at visible wavelengths—and silicon (Si), the leading material for microelectronic devices, is opaque in the visible portion of the electromagnetic spectrum. Silicon is, however, partially transparent at infrared (IR) wavelengths $\lambda > 1.1 \mu\text{m}$.

There are no temperature-sensitive fluorophores, to our knowledge, that emit at $\lambda > 900 \text{ nm}$ with good quantum yield (*i.e.*, the ratio of the energy of the emissions to that of the excitation) because the fraction of absorbed photons lost to nonradiative decay processes becomes significant at these longer wavelengths. The nanocrystals of semiconductor materials, known as quantum dots (QD), have a broadband absorption, yet a narrow emission (at least compared with typical fluorophores) due to quantum effects.⁵ And materials such as lead sulfide (PbS) emit at wavelengths of 0.8–1.8 μm with good quantum yield.⁶

Previous studies have already shown that the emissions from PbS core-shell quantum QD vary with temperature when embedded in glass or polymer matrices at temperatures up to 27 °C,^{7,8} but there is little known about the temperature sensitivity of PbS IRQD in

⁵ M. G. Bawendi, M. L. Steigerwald and L. E. Brus (1990) “The quantum mechanics of larger semiconductor clusters (‘quantum dots’)” *Ann. Rev. Phys. Chem.* **41**, 477

⁶ E. H. Sargent (2005) “Infrared quantum dots” *Adv. Mater.* **17**, 515

⁷ A. Olkhovets, R. C. Hsu, A. Lipovskii and F. W. Wise (1998) “Size-dependent temperature variation of the energy gap in lead-salt quantum dots” *Phys. Rev. Lett.* **81**, 3539

suspension at temperatures exceeding room temperature. Moreover, PbS QD have poor photostability because they are easily oxidized. This oxidation, which starts at the outer surface, reduces the effective size of the IRQD and hence reduces (“blue-shifts”) its emission (and absorption) wavelength range. Recently a new method has been developed to overcoat PbS QD with a cadmium sulfide (CdS) layer via a cation-exchange method; these overcoated QD were reported to have a useful life “under ambient conditions from a few days to at least several months, during which time the emission ... does not measurably shift in wavelength.”⁹

Experiments were therefore carried out to determine the temperature sensitivity of suspended CdS-overcoated PbS QD. These IRQD were synthesized by S. Geyer, a Ph.D. student in the group of Prof. M. G. Bawendi in the Chemistry Department at the Massachusetts Institute of Technology (MIT). A QD-toluene suspension at an absorbance $A = 0.45$ was excited at $\lambda = 488$ nm and continuously stirred at a constant temperature (Fig. 3). The energy of the emissions from the PbS QD in the near-IR at $\lambda = 1.25\text{--}1.84$ μm was measured by an indium gallium arsenide (InGaAs) photodiode at various suspension temperatures T , as measured by a thermocouple (TC).

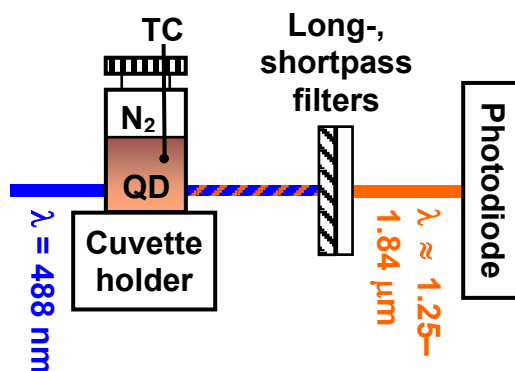


Figure 3. Experimental setup to measure the temperature sensitivity of the CdS-overcoated PbS QD suspension.

In each experiment, the IRQD suspension underwent four successive heating and cooling cycles over a total time of about 6 h where the suspension was heated from nominal temperatures of 20 °C to 60 °C, then cooled back down to 20 °C in 10 °C increments. Fifty samples of the energy of the IRQD emissions over an interval of 17 ms were obtained at 5 Hz, and the average energy E and standard deviation in the energy of the IRQD emissions were calculated over these samples. The average energy was then normalized by the maximum value E_{ref} within a single cycle (since the time interval for a single heating and cooling cycle of ~ 1.5 h is comparable to the typical timespan of an actual thermometry experiment) which was observed at a temperature $T_{\text{ref}} = 19.3 \pm 0.1$ °C. To evaluate the photostability of these temperature tracers, the emissions of the suspension were measured for the suspension under nitrogen (N_2) gas, under air, and after the suspension was under N_2 for up to 103 days.

Education and Outreach Activities

In the summer of 2010, Dr. Yoda worked with Dr. Chanley Small, Juliet Allan and Valerie Bennet, science teachers at a local high school, Westminster High School, to

⁸ C. Liu, Y. K. Kwon and J. Heo (2008) “Laser-induced blue-shift of the photoluminescence from PbS quantum dots in glasses” *Chem. Phys. Lett.* **452**, 281

⁹ J. M. Pietryga, D. J. Werder, D. J. Williams, J. L. Casson, R. D. Schaller, V. I. Klimov and J. L. Hollingsworth (2008) “Utilizing the lability of lead selenide to produce heterostructured nanocrystals with bright, stable infrared emission” *J. Am. Chem. Soc.* **130**, 4879

create a new program that involved students between their Junior and Senior years in research projects with various faculty in the School of Mechanical Engineering at GT. Seven (four female, three male) students from Westminster and Paces Academy worked with four different faculty on projects ranging from evaluating cookstoves powered by rice husks suitable for developing countries to developing agent-based computational models of cell differentiation in mammalian embryos. One of the (female) students from Westminster, Anjali Bhatia, worked with C. R. Dietz and Dr. Yoda (who served as the faculty advisor on this project while Dr. Joshi was on sabbatical at the Catholic University of Leuven in Belgium) on evaluating how various fabrication protocols changed the composition of the cupric hydroxide $[\text{Cu}(\text{OH})_2]$ and copper oxide $[\text{CuO}]$ nanostructures described previously. We plan to continue this high school research program next summer.

Elizabeth L. Elbel, an undergraduate student in Mechanical Engineering, also worked with C. R. Dietz and Dr. Joshi on a research project evaluating fabrication protocols for $\text{Cu}(\text{OH})_2$ and CuO nanostructures as part of ME 4699, Research Problems.

Dr. Joshi has also been involved in K-12 outreach during the four-year period of this proposal by:

- Serving as a Special Awards Judge in May 2008 at the Intel International Science and Engineering Fair (ISEF), the world's largest pre-college science competition; and
- Hosting Mr. Varun Gopinath, currently a student at Wheeler High School in Marietta, GA, as a Georgia Tech Center for Education Integrating Science, Math and Computing (CEISMIC) intern this summer (2009).

Research Findings

This section summarizes the research findings over the four-year-period of this grant for:

- dual-tracer fluorescent thermometry (DFT) and evanescent-wave fluorescence thermometry (EFT) measurements of liquid and wall surface temperatures in Poiseuille flow through heated channels with strong temperature gradients;
- visualizations of the initial phases of water condensing on superhydrophobic surfaces with nanoscale copper nanowires and bare silicon surfaces under vacuum in an environmental scanning electron microscope (ESEM);
- the temperature sensitivity and photostability of the near-IR emissions from CdS-overcoated PbS QD.

We then conclude with a list of the presentations and publications from this work.

DFT and EFT in Heated Channels

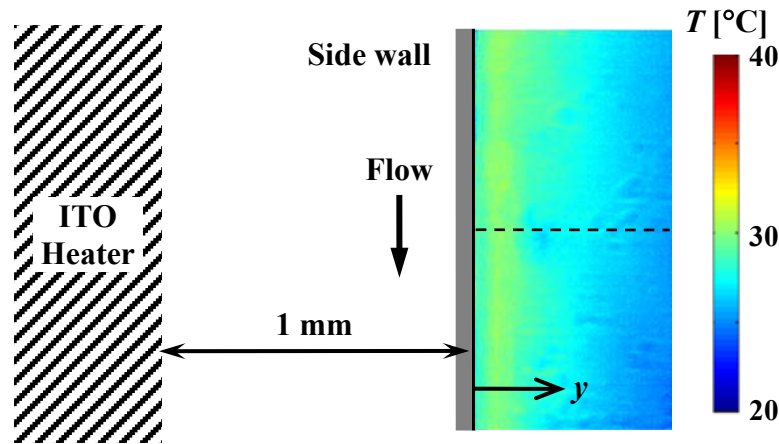


Figure 4 Pseudocolor temperature distribution in the water near the heated channel side wall obtained with DFT at $Re = 8.3$.

Figure 4 shows the temperature field obtained using DFT from the ratio of the FI and SrB emissions over a $0.95 \text{ mm} \times 0.445 \text{ mm}$ (650×320 pixel) “slice” of the Poiseuille flow at the higher flowrate studied, or $Re = 8.3$, through the heated channel near the bottom (glass) wall. The location of the ITO heater and the side wall of the channel are shown in the Figure to the left of the temperature data. Figure 5 shows water temperature profiles T as a function of the normalized coordinate y/L along the dashed line shown in Figure 4 (*triangles*). Here, y is measured across the channel from the side wall nearest the ITO heater, and $L = 1 \text{ mm}$ is the channel width. These data are compared with the FLUENT predictions for the temperature profile at the wall surface (*circles*) and those at the node nearest the wall, or $50 \text{ }\mu\text{m}$ from the wall (*squares*) at (a) $Re = 3.3$ and (b) $Re = 8.3$. The DFT data in the Figure are averaged over a 20 pixel square region, and hence have a spatial resolution of $30 \text{ }\mu\text{m}$ in the plane of the image. The error bars denote the uncertainty of $0.21 \text{ }^\circ\text{C}$ in the DFT results.

As expected, the temperatures are maximum near the heater, then drop by 4–5 °C over about 0.45 mm, corresponding to a temperature gradient of 9.2–9.9 °C/mm along y just above the glass wall. The temperature gradient along z in the same region of the flow is about 1.5 °C/mm based on the FLUENT simulations.

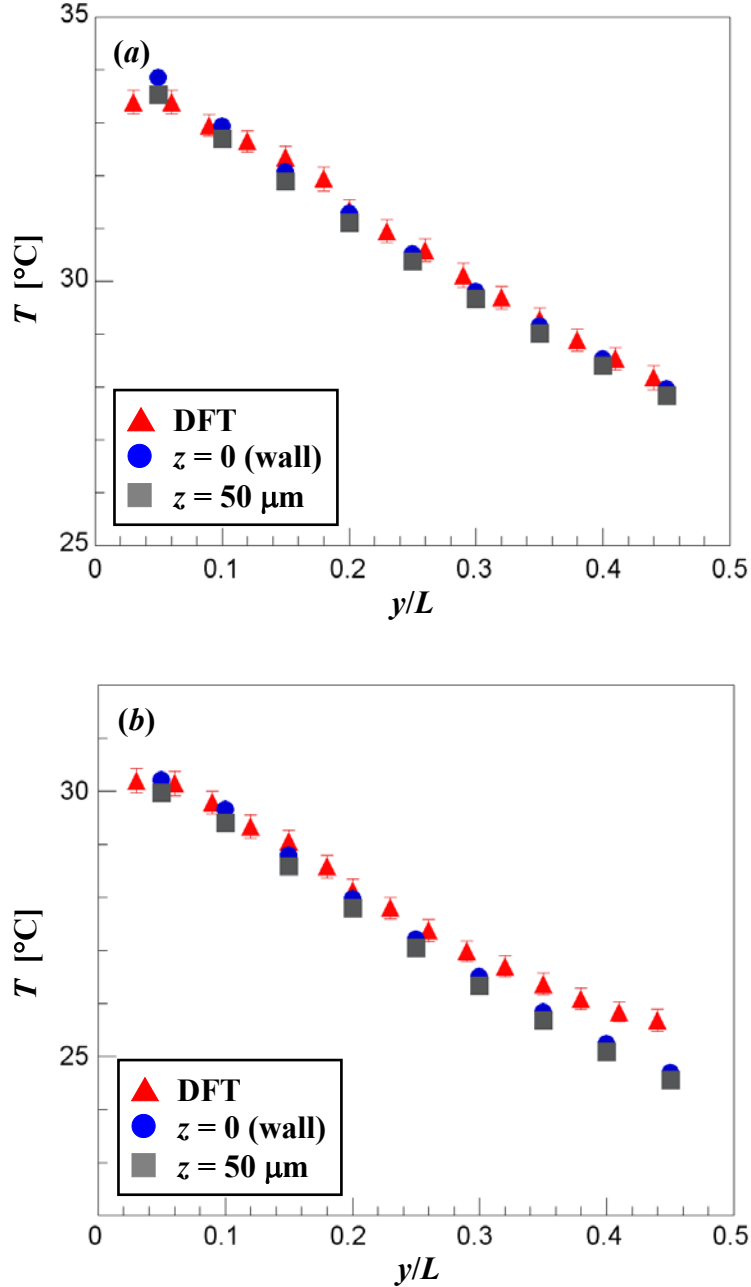


Figure 5 Fluid temperature T measured using DFT over a physical distance of 0.5 mm as a function of normalized channel coordinate y/L (\blacktriangle) compared with the values predicted by FLUENT at the wall, or $z = 0$ (\bullet) and at $z = 50 \mu\text{m}$ (\blacksquare) at (a) $Re = 3.3$ and (b) $Re = 8.3$.

The temperature results shown here should therefore lie between the FLUENT results at $z = 0$ and $50 \mu\text{m}$. Although the spatial resolution of the FLUENT results of $50 \mu\text{m}$ is still

greater than the $30\text{ }\mu\text{m}$ resolution of the DFT data, they and numerical predictions are in reasonable agreement: the average discrepancy between the DFT results and a cubic polynomial curve-fit of the numerical predictions at $z = 0$ is $0.22\text{ }^\circ\text{C}$ and $0.35\text{ }^\circ\text{C}$ at $Re = 3.3$ and 8.3 , respectively. The average discrepancy is greater at the higher Re because the numerical simulations consistently underpredict the DFT results for $y/L \geq 0.2$, where $T < 28\text{ }^\circ\text{C}$. This discrepancy may be due to low signal-to-noise ratios (SNR) in the FI images at lower T because the FI emissions decrease at lower T , where this noise will then affect the ratio of the FI and SrB signals used to estimate T . Nevertheless, the accuracy of these data are an improvement over recent DFT studies in microchannels using RhB and sulforhodamine B which have reported uncertainties as small as $0.5\text{ }^\circ\text{C}$ at a (slightly finer) spatial resolution of $22\text{ }\mu\text{m}$.¹⁰

Figure 6 shows the temperature field obtained using EFT from the FI emissions over a $100\text{ }\mu\text{m} \times 120\text{ }\mu\text{m}$ (410×500 pixel) region of the Poiseuille flow at $Re = 3.3$ within the first 320 nm next to the bottom wall. The location of the ITO heater and the channel side wall are again shown on the left. The diffraction patterns visible in the Figure are typical of evanescent-wave illumination from a TIRF microscope. Figure 7 compares water temperature profiles T along the dashed line shown in Figure 6 (*triangles*) as a function of the normalized coordinate across the channel y/L at $Re = 3.3$ (a) and 8.3 (b). The EFT data, which are averaged over 40 pixels and hence have a spatial resolution of $10\text{ }\mu\text{m}$ in the plane of the image, are compared with numerical predictions at the wall (*circles*), or $z = 0\text{ }\mu\text{m}$, and at $z = 50\text{ }\mu\text{m}$ (*squares*). The fluctuations in the EFT results are likely due to the diffraction patterns, while the error bars represent the uncertainty of $0.16\text{ }^\circ\text{C}$.

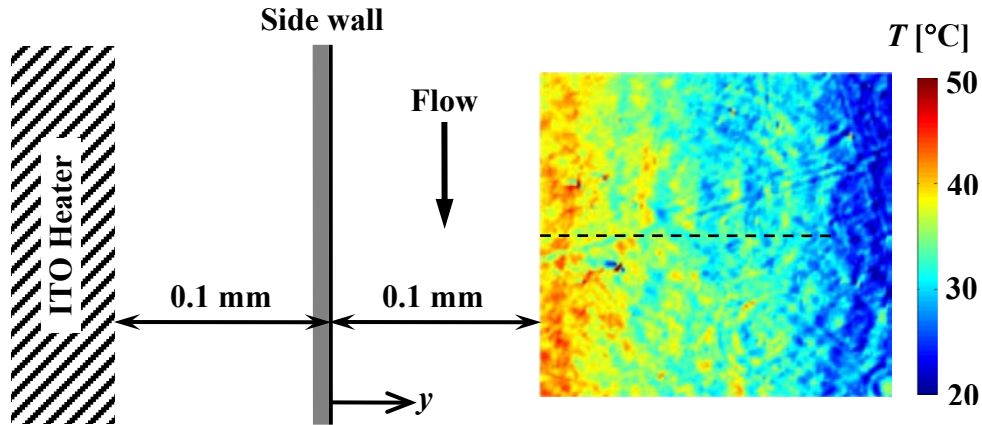


Figure 6 Pseudocolor temperature map at $Re = 3.3$ over a $100\text{ }\mu\text{m} \times 120\text{ }\mu\text{m}$ region obtained using EFT for the water within the first 320 nm of the glass channel wall at a spatial resolution of $1\text{ }\mu\text{m}$.

The EFT data should have a spatial resolution of about $0.3\text{ }\mu\text{m}$ along z (*i.e.*, normal to the image plane). There is good agreement between the EFT results and the FLUENT predictions at the wall, with an average discrepancy of $0.63\text{ }^\circ\text{C}$ (based again on a cubic

¹⁰ V. K. Natrajan and K. E. Christensen (2010) “Non-intrusive measurements of convective heat transfer in smooth- and rough-wall microchannels: laminar flow” *Exp. Fluids* **49**, 1021

polynomial curve-fit of the numerical predictions at $z = 0$). Given how rapidly the fluid temperature changes along z , decreasing by about 4–6 °C over a distance of 50 μm , these results suggest that the EFT results are a good estimate of the wall surface temperature.

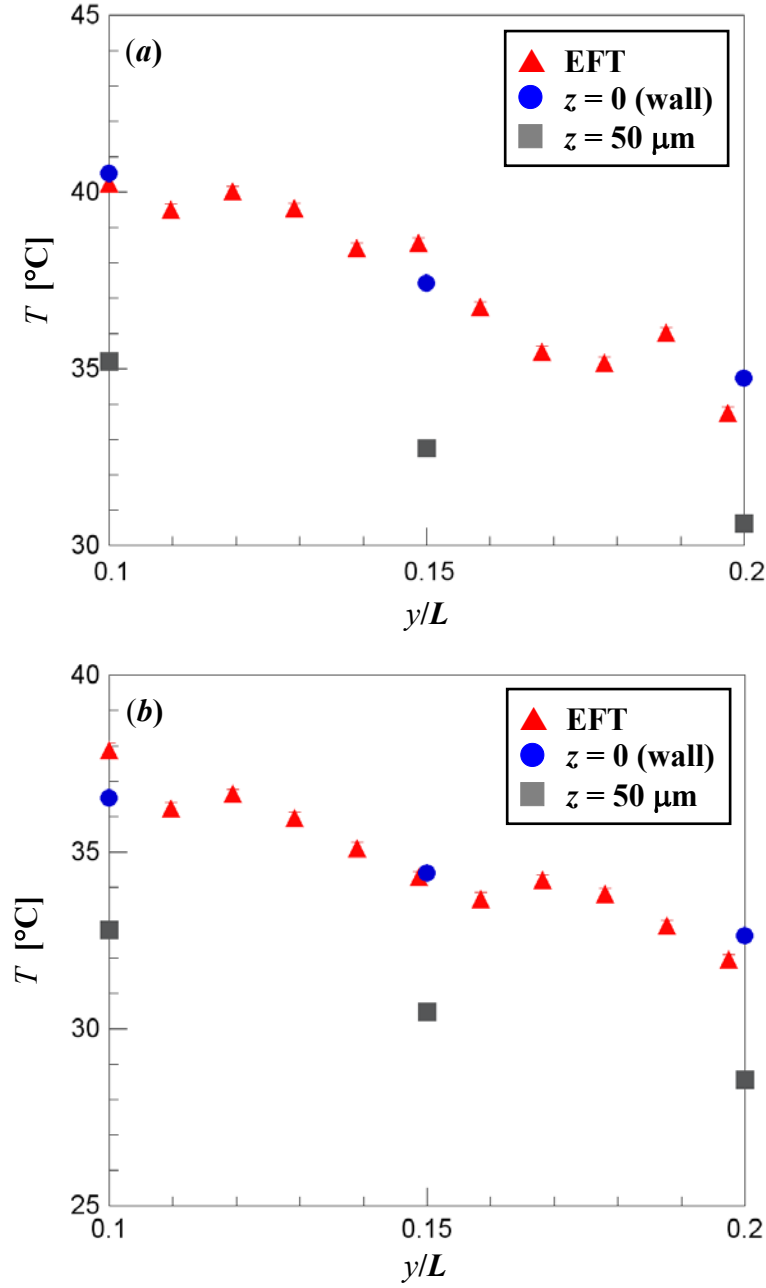


Figure 7 Fluid temperatures T as a function of normalized channel coordinate y/L over a 100 μm segment of the channel measured by EFT (\blacktriangle) compared with numerical predictions at $z = 0$ (\bullet) (*i.e.*, the wall) and $z = 50 \mu\text{m}$ (\blacksquare) for $Re = 3.3$ (a) and 8.3 (b).

Studies of Condensation over Nanostructured Surfaces

Representative ESEM images of condensation on two nanostructured surfaces are shown in Figure 8. On the $\text{Cu}(\text{OH})_2$ nanostructured surface, the droplets rapidly start to roll off as the condensate begins to coalesce, sweeping other drops in their path (gravity acts towards the top of the images). Figures 8a and 8c show a cluster of droplets before coalescence at 1 min and 4 min into the experiment, respectively. After the coalescence, these areas are swept clean by the droplets rolling off of the surface as seen in the next set of images taken a few seconds later (Fig. 8b and 8d). On the non-structured Rain-X surface, the droplets do not roll, and hence continue to grow, as can be seen by comparing images taken at 1 min (Fig. 8e) and 4 min (Fig. 8f). Later, at times beyond 4 min, the non-structured surface was observed to become completely flooded by the condensate, while the $\text{Cu}(\text{OH})_2$ nanostructured superhydrophobic surface continued to shed drops.

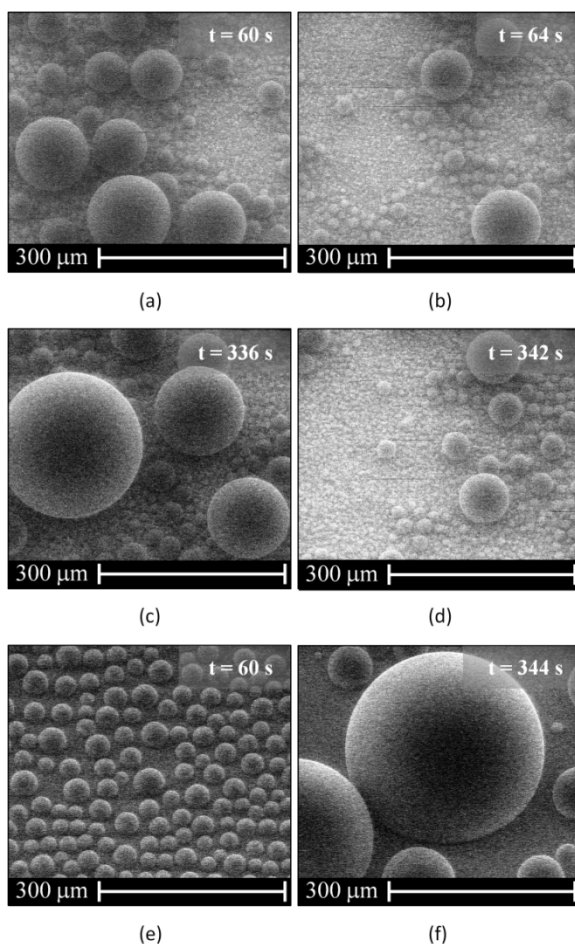


Figure 8 ESEM images of dropwise condensation at different times for (a–d) a $\text{Cu}(\text{OH})_2$ nanostructured superhydrophobic surface and (e–f) a Rain-X coated non-structured surface.

Figure 9 shows representative data on the number of nucleated droplets as a function of time for the two surfaces. Although the number of droplets at any given time varies between runs due to the variation in condensate nucleation sites based on the location of the ESEM focal point, the observed qualitative trends were consistent over all the experimental runs. Since the droplets roll off of the $\text{Cu}(\text{OH})_2$ nanostructures, the

condensation state fluctuates between a few large droplets and many small droplets, and these fluctuations persist over the entire duration of the condensation visualizations. On the Rain-X coated non-structured silicon surfaces, however, the droplets do not roll off, and the droplet number steadily decreases as time increases. The data are further analyzed by plotting a histogram of the droplet diameter over 60 s time intervals for both surface types (Fig. 10). For the $\text{Cu}(\text{OH})_2$ nanostructures, the percentage of the droplets formed that have diameters less than $10\text{ }\mu\text{m}$, and are hence the droplets that contribute the most to condensation heat transfer, is fairly consistent over each 60 s time interval is . In the first minute, about 21% of all such droplets are formed for the entire experiment, while about 22% of all such droplets are formed during the fourth minute. For the Rain-X coated non-structured silicon surfaces, however, about 89% of the droplets smaller than $10\text{ }\mu\text{m}$ are formed during the first minute of condensation, and fewer and fewer such droplets are formed as the experiment progresses—indeed, only 4% of such droplets are formed during the fourth minute of the experiment.

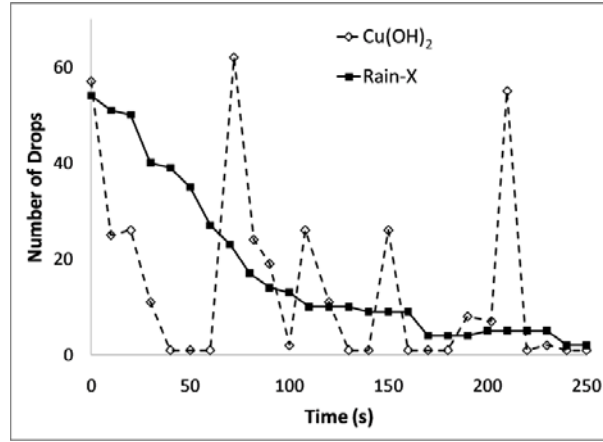


Figure 9 Plot comparing the number of drops in an image as a function of time for a Rain-X coated non-structured silicon surface and a $\text{Cu}(\text{OH})_2$ nanostructured surface.

Since the $\text{Cu}(\text{OH})_2$ surface is able to continuously form and shed small droplets, these surfaces could potentially have greater heat transfer coefficients during dropwise condensation. On a non-structured hydrophobic surface, water drops must typically grow to 2-3 mm in diameter before they begin to slide on a vertical surface. From the results presented in this study, the average drop departure size on the superhydrophobic surface, when tilted at 30° with respect to the horizontal, was about $300\text{ }\mu\text{m}$. By balancing the gravitational and surface tension forces, the average drop departure size for the superhydrophobic surface, when vertical, is estimated to be $\sim 250\text{ }\mu\text{m}$, about an order of magnitude less than that required for the non-structured surface.

Rose and Le Fevre¹¹ proposed a distribution of condensed water drop sizes for a vertical surface

$$A(r) dr = \frac{1}{3} \left(\frac{\hat{r}}{r} \right)^{1/3} \frac{dr}{\hat{r}} \quad (1)$$

¹¹ E. J. Le Fevre and J. W. Rose (1965) "An experimental study of heat transfer by dropwise condensation" *International Journal of Heat and Mass Transfer* **8**, 1117

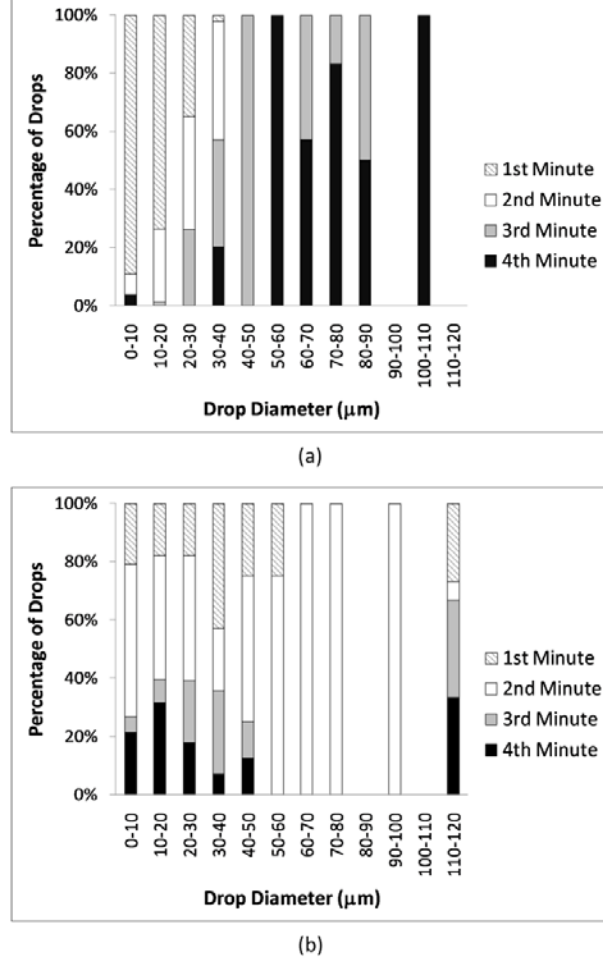


Figure 10 Histogram of drop diameters, averaged over 60 s intervals, for (a) the Rain-X coated non-structured surface and (b) a Cu(OH)₂ nanostructured surface.

where $A(r)$ is the fractional surface area covered by droplets with radius between r and $r+dr$, and \hat{r} is the maximum droplet radius defined semi-empirically as the ratio between surface tension and gravitational forces. The heat transfer through a single droplet of a given radius r can be viewed as a resistance network where the driving potential is the temperature difference between the saturated vapor and the surface, less the amount the vapor needs to be sub-cooled on account of the drop surface curvature. The total resistance is then the sum of the resistance due to conduction through the drop and that due to interfacial mass transfer. By integrating the heat transfer through a single drop over the drop distribution the following integral for the average heat flux q is obtained:

$$q = \frac{1}{3\hat{r}^{1/3}} \int_r^{\hat{r}} \left(\Delta T - \frac{2\sigma T}{r\rho h_{fg}} \right) \left/ \left[\frac{2r}{3k} + \frac{0.627}{1.328} \frac{T}{h_{fg}^2 \rho_v} \left(\frac{\gamma+1}{\gamma-1} \right) \left(\frac{R_g T}{2\pi} \right)^{1/2} \right] \right. \frac{dr}{r^{2/3}} \quad (2)$$

where ΔT is the surface subcooling, T is the saturation temperature, σ is the surface tension, ρ and ρ_v are the liquid and vapor densities, respectively, h_{fg} is the heat of

vaporization, k is the liquid thermal conductivity, γ is the ratio of specific heats, and R_g is the specific ideal-gas constant. The maximum droplet radius used by Rose and Le Fevre was of the order of 2 mm. By replacing the maximum drop radius with the estimated maximum drop size for a vertically aligned $\text{Cu}(\text{OH})_2$ superhydrophobic surface of 0.25 mm, the increase in the heat flux for this surface can be determined. Equation 2 suggests that the vertically oriented superhydrophobic nanostructured surface should yield about a 100% increase in the heat transfer coefficient during dropwise condensation compared to a vertically oriented non-structured hydrophobic surface with the same temperature difference between the saturated vapor and the surface.

Temperature Sensitivity of Infrared Quantum Dots

Figure 11 shows E / E_{ref} , the average emission energy from the PbS/CdS core-shell QD suspended in toluene normalized by its maximum value within a single heating/cooling cycle, as a function of $\Delta T \equiv T - T_{\text{ref}}$, the difference between the actual solution temperature and the temperature where E_{ref} occurs. Results are presented over all four heating and cooling cycles for the same sample 1 day (+), 100 days (O) and 103 days (\diamond) after suspension, as well as for a different sample 1 day after suspension (\times). In all cases, the samples were stored under N_2 after suspension. In all cases, the standard deviation in E / E_{ref} is smaller than the symbols. The results show that the temperature response of the PbS/CdS IRQD remains consistent over several weeks, even in a fairly dilute suspension, and that the results are reproducible for different PbS/CdS QD samples. A linear curve-fit (with $R^2 = 0.982$) to all four sets of data, denoted by the dashed line, gives:

$$\frac{E}{E_{\text{ref}}} = 1.00 - \frac{4.98 \times 10^{-3}}{^\circ\text{C}} \Delta T \quad (3)$$

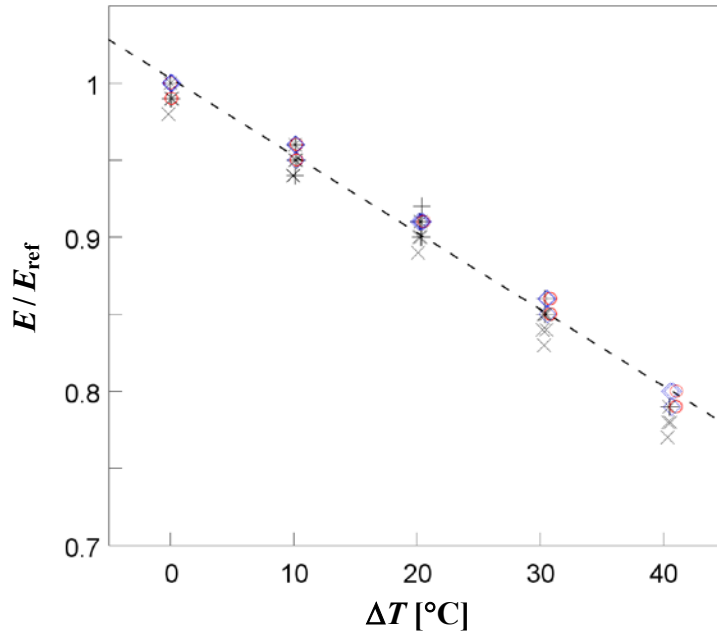


Figure 11 Average normalized IR emission energy as a function of the temperature difference ΔT for PbS/CdS quantum dots suspended in toluene and stored under N_2 for 1 (\times and $+$), 100 (\circ), and 103 (\diamond) days. The maximum standard deviations for these data are smaller than the symbols. The curve-fit given by Eq. (3) is shown by the dotted line.

As shown in the Figure, the temperature sensitivity of the IRQD after 1, 100, or 103 day(s) remains essentially constant. However, it appears that the emissions are slightly stabilized by storage under N_2 for more than a day. The average standard deviations in E/E_{ref} for the samples after 1 day, 100 days and 103 days were 0.14%, 0.08% and 0.08%, respectively, corresponding to average uncertainties in the temperature results, based on Eq. (3), of 0.2–0.3 °C. Similar results (not shown here) were obtained for the IRQD emissions imaged through a 0.38 mm thick lightly doped silicon wafer.

Although results are not shown here, our studies also showed that the PbS/CdS core-shell QD have nearly identical temperature response, both in terms of E/E_{ref} and its standard deviation, after one day as a suspension in toluene under N_2 or air. This suggests that these IRQD are so resistant to oxidation that they can be stored, even as a fairly dilute colloidal suspension, under air for several hours, greatly simplifying their use as a temperature tracer.

In summary, these studies show that CdS-overcoated PbS quantum dots with emissions centered around 1.35 μm can be stored as a relatively dilute colloidal suspension under air for at least 1 day and under nitrogen for more than 100 days with no noticeable degradation in their temperature sensitivity. Moreover, the uncertainty in the liquid temperatures estimated from the emissions of these tracers is no more than 0.3 °C, a value comparable to that of commercial thermocouples.

Publications and Presentations from this Grant

In terms of dissemination of this research, this work has resulted in seven journal publications (five published, two submitted):

- 1) Dietz, C. D. and Joshi, Y. K. “Single-phase forced convection in microchannels with carbon nanotubes for electronic cooling applications,” *Nanoscale and Microscale Thermophysical Engineering* **12**, 251–271 (2009)
- 2) Im, Y., Joshi, Y., Dietz, C. and Lee, S. S. “Enhanced boiling of a dielectric liquid on copper nanowire surfaces,” *International Journal of Micro-Nano Scale Transport* **1**, 79–96 (2010)
- 3) C. Dietz, K. Rykaczewski, A. G. Fedorov and Y. Joshi “Visualization of droplet departure on a superhydrophobic surface and implications to heat transfer enhancement during dropwise condensation,” *Applied Physics Letters* **97**, 033104/1–3 (2010)
- 4) C. Dietz, K. Rykaczewski, A. Fedorov and Y. Joshi “ESEM imaging of condensation on a nanostructured superhydrophobic surface,” *Journal of Heat Transfer Transactions of the ASME* **132**, 080904/1 (2010)
- 5) Kim, M. and Yoda, M. “Dual-tracer fluorescence thermometry measurements in a heated channel,” *Experiments in Fluids* **49**, 257–266 (2010)
- 6) Kim, M. and Yoda, M. “Fluorescence thermometry for measuring wall and bulk liquid temperatures,” submitted to *Journal of Heat Transfer Transactions of the ASME* (2010)

- 7) Kim, M. and Yoda, M. “Infrared quantum dots for liquid-phase thermometry in silicon,” submitted to *Measurement Science and Technology* (2010)

as well as three refereed conference papers:

- 1) Kim, M. and Yoda, M. “Infrared quantum dot thermometry for liquid-phase measurements in silicon microchannels” ASME paper HT2008-56207, American Society of Mechanical Engineers Summer Heat Transfer Conference, Jacksonville, FL (2008)
- 2) Kim, M. and Yoda, M. “Fluorescence thermometry for measuring wall surface and bulk fluid temperatures” ASME paper IHTC14-22884, Proceedings of the 14th International Heat Transfer Conference, Washington, DC (2010)
- 3) Kim, M. and Yoda, M. “Using quantum dots for liquid-phase thermometry at near-infrared wavelengths in silicon devices” ASME paper IHTC14-22885, Proceedings of the 14th International Heat Transfer Conference, Washington, DC (2010)

The results from this work have also been featured in two invited talks at national and international conferences:

- 1) M. Yoda and H. F. Li “Experimental Techniques for Validating Nano/Microfluidic Models,” 10th US National Congress on Computational Mechanics (USNCCM-X), Columbus, OH, July 16–19 (2009)
- 2) M. Yoda “Interfacial Velocimetry and Microscale Thermometry,” Horiba International Symposium on Micro/Nano Flow Measurement Techniques (Tokyo, Japan), Sept. 20–22 (2010)

Finally, Myeongsub Kim, who was supported by this grant, will be completing his Ph.D. thesis in December 2010, titled *Microscale Optical Thermometry Techniques for Measuring Liquid-Phase and Wall Surface Temperatures*.